MedChemComm

Accepted Manuscript

ROYAL SOCIETY OF CHEMISTRY

www.rsc.org/medchemcomm

Synthesis

R=

-C(O)-O-CH_2-CH_2-CH_3
-C(O)-O-CH_2-CH_2-CH_2-CH_3
-C(O)-O-CH_2-CH_2-CH_2-CH_2-CH_3
-C(O)-O-CH_2-CH_2-CH_2-CH_2-CH_2-CH_3
-C(O)-O-CH_2-CH_2-CH_2-CH_2-CH_2-CH_2-CH_3

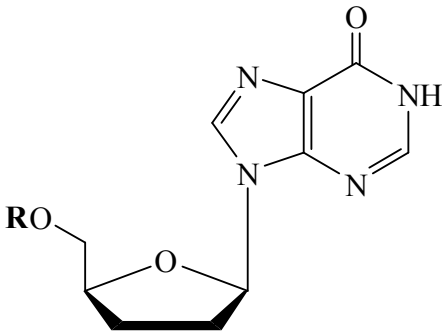

In vitro anti-HIV activity and cytotoxicity

Ability to bind to the citoplasmatic 5'-nucleotidase (ncN-II)

Biological evaluation and molecular modelling of didanosine derivatives

Soledad Ravetti,[1] Cristian A De Candia,[2] María S Gualdesi,[1] Sandra Pampuro,[2] Gabriela Turk,[2] Mario A Quevedo,[1] Margarita C Briñón.[1,*]

[1]Departamento de Farmacia, Facultad de Ciencias Químicas, Ciudad Universitaria, Universidad Nacional de Córdoba, 5000 Córdoba, Argentina. Tel: +54-351-5353865; Fax: +54-351-4334127.

[2]Instituto de Investigaciones Biomédicas en Retrovirus y SIDA, INBIRS, Facultad de Medicina, Universidad de Buenos Aires, Argentina.

Running head

Synthesis and anti-HIV activity of novel didanosine prodrugs

Keywords: didanosine carbonates, prodrugs, anti-HIV activity, cytotoxicity, molecular docking, molecular dynamics.

ABSTRACT

Five carbonate derivatives of 5´-*O*-2´,3´-dideoxyinosine (DDI, **1**) have been synthesized by combination with aliphatic alcohols, with their *in vitro* anti-HIV activity and cytotoxicity, being afterward evaluated in human peripheral blood mononuclear cells (PBMCs). One particular compound, namely DDI-Penta exhibited an outstanding performance because it was found to have both a higher inhibitory potency and a lower cytotoxicity than the lead compound, resulting in a 100x enhancement in its selectivity index. In order to further study this phenomenon, the ability of these derivatives to bind to the cytoplasmic 5'-nucleotidase (ncN-II) was studied by *in-silico* methods. Also, the higher calculated lipophilicity of the synthesized compounds was proposed to improve their permeability through the cell membrane since said lipophilicity would allow a higher concentration of the corresponding prodrug inside the infected cell. Overall, a combination of an optimal lipophilicity and the ability of DDI-Penta to bind to ncN-II are suggested due to the higher potency and lower cytotoxicity observed for this compound. Based on the reported findings, we believe that the combination of certain aliphatic alcohols and DDI through a carbonate linkage could significantly increase the performance of this class of therapeutic compounds; therefore, it merits further evaluations.

*Corresponding author. E-mail: macribri@fcq.unc.edu.ar

Highlight: These prodrugs of DDI with increased lipophilicity and good antiviral performance should be of interest in HIV therapy.

1. Introduction

Since first reported in the 1980s, type-1 human immunodeficiency virus (HIV-1) has spread rapidly through the human population and become one of the most devastating infectious agents facing mankind.[1-2] HIV-1 is the etiologic agent that causes Acquired Immunodeficiency Syndrome (AIDS) which results in life-threatening opportunistic infections and malignancies. The increasing incidence of resistance to anti-HIV drugs together with many serious side effects and long-term complications for patients decrease the efficacy of the therapeutic compounds currently in use, which justifies the search for novel antiviral agents.[1-2]

Didanosine (2´,3´-dideoxyinosine, DDI, Figure 1.a) is a nucleoside reverse transcriptase inhibitor (NRTI),[3] which is usually used in combination with other antiviral agents like zidovudine (AZT, Figure 1.b) and lamivudine (3TC, Figure 1.c) in the Highly Active Antiretroviral Therapy (HAART) against HIV-1 infection in adults. After reaching the cell cytoplasm, DDI is first phosphorylated by a nucleotidase enzyme to form DDI-5'-monophosphate (DDI-MP),[4] with 5'-nucleotidase ncN-II (ncN-II) identified as the main protein isoform involved that has been vastly characterized and studied from a biochemical and structural point of view.[5-6] In a second step, DDI-MP is converted to dideoxyadenosine-5'-monophosphate (DDA-MP) by adenylosuccinate synthetase and lyase, with subsequent phosphorylation to DDA-5'-triphosphate (DDA-TP) by adenylate kinase (miokinase). DDA-TP constitutes the active metabolite that is responsible for the inhibition of the viral reverse transcriptase, acting as a competitive inhibitor or alternative substrate unlike the normal ones which leads to the termination of viral DNA chain elongation.[7-9] However, DDI exhibits several pharmacokinetic disadvantages like short plasma half-life (≈ 1h), relative low bioavailability, and a limited penetration into the central nervous system.[10-12]

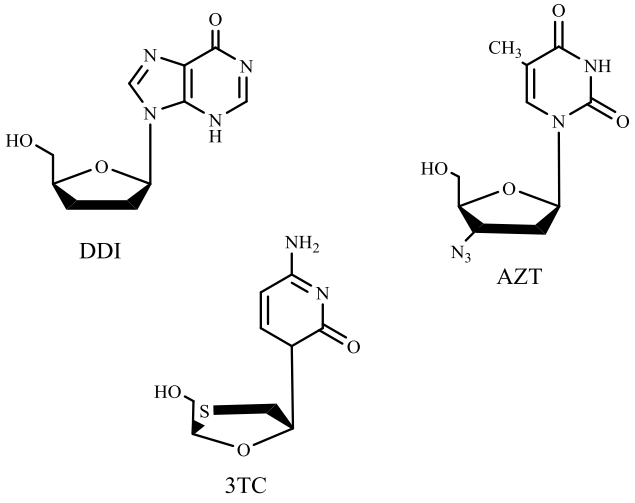

Figure 1. Chemical structures of: a) didanosine (DDI), b) zidovudine (AZT) and c) lamivudine (3TC).

The design of prodrugs is one of the methods selected to improve the anti-HIV efficacy of a drug molecule by enhancing its spectrum of chemotherapeutic properties for the effective treatment of AIDS. The mentioned prodrugs would lead to a major distribution and retention of the parent compound in the body for a longer time.[13-15] Thus, the prodrugs have been rationally designed to decrease the toxicity associated with nucleoside drugs, to release active species from their degradative metabolisms and to allow larger amounts of drug to enter the cell.[13,16-20] Although several DDI prodrugs have been prepared and evaluated *in vitro* and *in vivo* to overcome some of these problems, none of them are currently in routine clinical use.[21]

Many nucleoside analogues with interesting biological properties have been developed by substitution at the 5'-*O* position of the NRTI with lipophilic chemical moieties linked by enzymatically hydrolysable functions such as ester and carbonate bonds.[19-27] The lipophilic character of the side chains at the 5´-*O* position should influence their ability to cross the cell membrane by passive diffusion, which is a key feature in the absence of an active nucleoside transport system.[22-24,28-29] As stated by Parang *et al*,[20] more selective compounds can be designed by using the strategy of 5'-*O*-carbonates substitution. Although the clinical application of these approaches remains unknown, they hold the promise of becoming an important tool in the treatment of HIV infection and its related consequences.

Recently, we synthesized and evaluated the anti-HIV activity of carbonate prodrugs of lamivudine (3TC) with the aim of generating 3TC derivatives that were able to suppress HIV-replication more efficiently than its parent drug, with some promising results being reported.[30] Therefore, as part of our ongoing efforts to search novel antiviral agents,[28, 30-34] we also used the 5'-*O*-carbonate substitution strategy to link the aliphatic alcohols on the 5´-*O* position of DDI in order to enhance their lipophilicity, to facilitate their diffusion through the cell membrane independently of the nucleoside transport system, and to improve the *in vitro* anti-HIV activity of DDI.[35-36]

2. Results and Discussion

2.1. Chemistry

Since the synthesis of 3TC prodrugs with ethanol, *n*-butanol, *n*-pentanol and *n*-hexanol moieties has previously demonstrated to be the most active compounds of the series against HIV[30] and HBV[37] viruses, in this work the synthetic protocols were extended to obtain the corresponding prodrugs of DDI. In addition, the synthesis of the prodrug including *n*-heptanol is first reported with the aim of including an additional methyl moiety in the explored series of *n*-alcohols.

Taking into account that didanosine (DDI, **1**, Figure 2) has one primary reactive functional group such as 5'-OH, an imidazole carboxylic ester, *N*, *N*-carbonyldiimidazole (CDI, **2**, Figure 2) was used in the controlled and selective formation of carbonate derivatives of DDI. Thus, in the current study, our synthesis strategy was focused on the association of 5´-OH of DDI with the selected aliphatic alcohols.[29-30, 36] This strategy was achieved in a two-step reaction sequence (Figure 2).

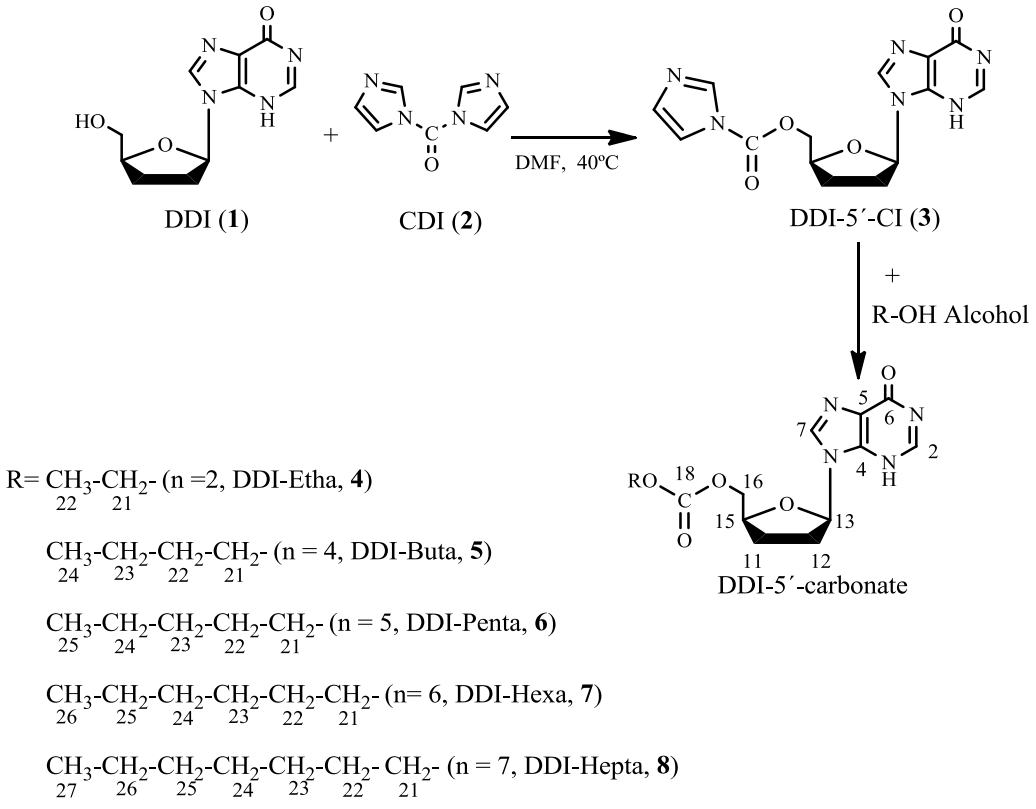

Figure 2. Synthetic protocol for the obtaining the novel DDI derivatives and chemical structures of didanosine (1, DDI) and their derivatives (4-8).

The didanosine intermediate named DDI-5'-CI (**3**, Figure 2) was obtained in quantitative yields by refluxing DDI with CDI in a dry mixture with dimethylformamide (DMF) at 40 °C for one hour.

As figure 2 shows, the *in situ* reaction of DDI-5'-CI with the respective aliphatic alcohols, ethanol, *n*-butanol, *n*-pentanol, *n*-hexanol and *n*-heptanol then gave the corresponding carbonates in 80-95% yields called 2´,3´-dideoxyinosine-5´-yl *O*-ethyl (DDI-Etha, **4**), 2´,3´-dideoxyinosine-5´-yl *O*-butyl (DDI-Buta, **5**), 2´,3´-dideoxyinosine-5´-yl *O*-pentyl (DDI-Penta, **6**), 2´,3´-dideoxyinosine-5´-yl *O*-hexyl (DDI-Hexa, **7**) and 2´,3´-dideoxyinosine-5´-yl *O*-heptyl (DDI-Hepta, **8**) carbonates, respectively. In all cases, unreacted DDI and CDI were not detected from the reaction media.

The reaction proceeds via the formation of an imidazole anhydride intermediate which decomposes after either intra- or internucleophilic attack by an imidazole group of CDI, as proposed by Rannard *et al*.[38-39] The purity of the synthesized compounds was checked by TLC and HPLC, and the structure of the resulting nucleoside derivatives **4-8** was identified by spectroscopic techniques such as ^{1}H-NMR, ^{13}C-NMR, DEPT 135 and COSY homo and heteronuclear spectra of **4-8,** being performed in DMSO-d_6. ^{1}H and ^{13}C-NMR (see Experimental Section).These techniques are in full agreement with the structures proposed for **4-8** (Figure 2), showing that their ^{1}H and ^{13}C resonances signals are characteristic of each of the moieties constituting structures of C-5' substituted pyrimidine nucleoside analogues (**4-8**).

In the ^{1}H-NMR spectra, the signals of the protons of these prodrugs were identified on the basis of their chemical shifts, multiplicities and coupling constants. The proton signals of H-2, H-8, H-1', H-2'and H-3' correlated well with those of DDI, while H-4' ($\delta\cong$ 4.10 ppm) and H-5' ($\delta\cong$ 3.50 ppm) showed certain chemical shift differences of about $\delta \cong 0.30$ ppm and $\delta \cong 0.40$ ppm, respectively, from the parent compound. Proton signals were successfully assigned using COSY homo (H-H) and heteronuclear (C-H) spectra.

The most significant features in the ^{13}C-NMR spectra of **4-8** were the signals at $\delta \cong$ 154-155 corresponding to the CO carbons from CDI. The rest of the^{13}C-NMR signals are also in concordance with those of DDI and the corresponding alcohols.

In the IR spectra of **4-8,** characteristic vibrational regions of the structural features were found.[40] The intensive absorption at 1690 cm^{-1} and 1744 cm^{-1} indicated the presence of carbonyl groups and the characteristic stretching of the carbonate moiety, respectively, as well as the characteristic of conjugation with the purine base. The hydrogen stretching region exhibits a broad band due to NH stretching bands and small C-H stretching bands. Other strong bands are the C-N stretching band at 1200 $cm^{-1}$and the C-O-C stretch of tetrahydrofurfuryl alcohol.

2.2. Antiviral and cytotoxicity evaluation

As previously described,[30,34] the reported DDI prodrugs (**4-8**) were evaluated *in vitro* for anti-HIV activity in a primary cultures of activated peripheral blood mononuclear cells (PBMCs) infected with HIV, with the corresponding inhibitory activities being compared to that of DDI as the reference standard. Assays on infected and uninfected PBMCs were performed in order to calculate the concentration of the drug that inhibits both 50% of viral replication (IC_{50}) and 50% of normal cell

growth ($CCID_{50}$), respectively. Selectivity indexes (SI = $CCID_{50}/IC_{50}$) were in turn calculated for each compound and compared to that of DDI. Results are shown in Figure 3 and summarized in Table 1.

a)

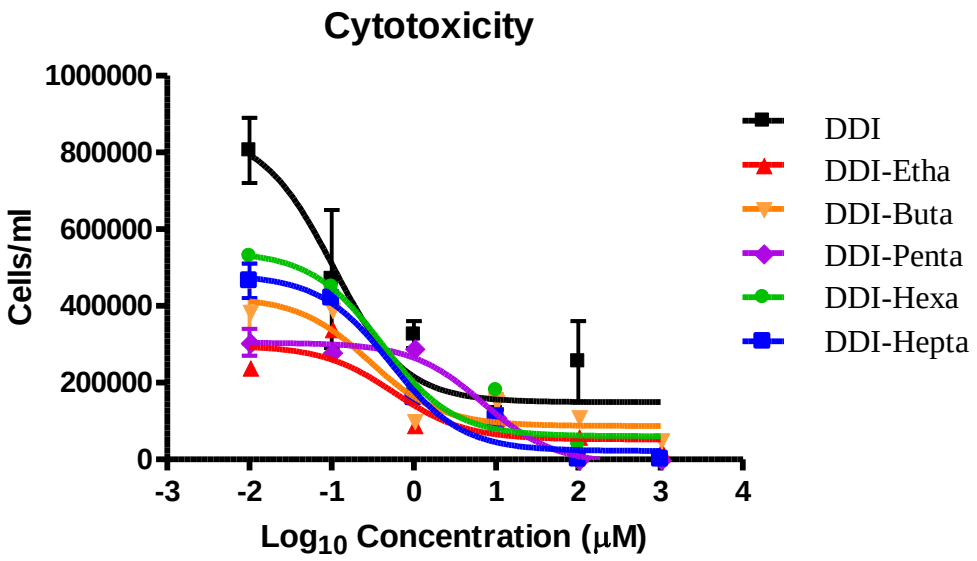

b)

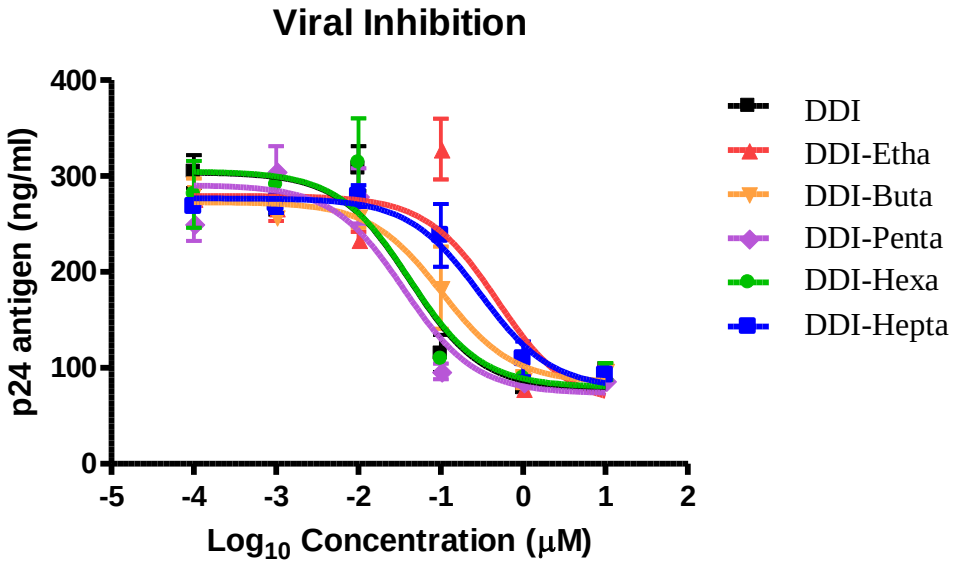

Figure 3. Cytotoxicity (A) and anti-HIV inhibitory effect (B) of DDI and its novel derivatives in PBMC. Dots represent the mean of three replicates ± SD. Lines represent the best-fit dose-response curves, calculated using GraphPad Prism 5.0 software.

Table 1. Anti-HIV activity, cytotoxicity and selectivity indexes (SI) of the DDI derivatives in PBMC[a].

Compound	$CCID_{50}$ (mM)[b]	IC_{50} (mM)[c]	SI[d]	clogP[e]
DDI	0.100±0.010	0.040±0.001	2.3±0.1	-1.92
DDI-Etha	0.570±0.0850	0.490±0.068	1.2±0.3	0.20
DDI-Buta	0.290±0.018	0.100±0.002	2.9±0.2	0.50
DDI-Penta	7.000±0.094	0.030±0.001	200±6	1.03
DDI-Hexa	0.220±0.004	0.040±0.001	5.2±0.2	1.56
DDI-Hepta	0.520±0.026	0.300±0.010	1.7±0.1	2.09

[a]PBMC = peripheral blood monocellular cell.
[b]$CCID_{50}$ = concentration of drug that inhibited 50% of cell growth.
[c]IC_{50} = concentration of drug that inhibited 50% of viral production.
[d]SI = Selectivity Index, defined as $CCID_{50}/IC_{50}$.
[e]clogP = Log P values obtained from the CLOGP program.

In uninfected PBMCs, the values of $CCID_{50}$ for the studied prodrugs followed the order: DDI < DDI-Hexa< DDI-Buta< DDI-Hepta< DDI-Etha< DDI-Penta. These compounds showed $CCID_{50}$ values similar or slightly higher to that of the parent drug. It is important to point out that DDI-Penta exhibited a marked increase in its $CCID_{50}$ (≈ 70-fold) compared to DDI, which indicates that this compound is significantly less cytotoxic than the parent drug. As regards IC_{50} values, DDI-Penta and DDI-Hexa exhibited similar antiviral potencies to DDI (i.e. showed similar IC_{50}), while the rest of the derivatives showed higher IC_{50} values. In turn, the SI values calculated for all the prodrugs were similar to that of DDI, with the exception of DDI-Penta for which a 100-fold higher SI was observed. This result is mainly driven by a combined high antiviral potency and a marked decrease in its cytotoxic effect, suggesting a selective and effective bioactivation of this particular prodrug within the PBMC cell.

In order to further characterize the anti HIV performance of DDI-Penta, its anti-HIV activity was evaluated in PBMCs infected with wild type (WT) and NRTI-resistant primary viral isolates (see Experimental section for details). The calculated IC_{50} and fold resistance (Fold-R!) values for DDI-

Penta and the parent drug were both similar (Figure 4, Table 2) when using WT or NRTI-resistant primary isolates. This indicates that DDI-Penta maintains similar antiviral effect against HIV laboratory-adapted and primary strains with less cytotoxicity if compared to DDI. As will be supported later in this manuscript, the above commented observations merit the continuity of the investigation into this derivative.

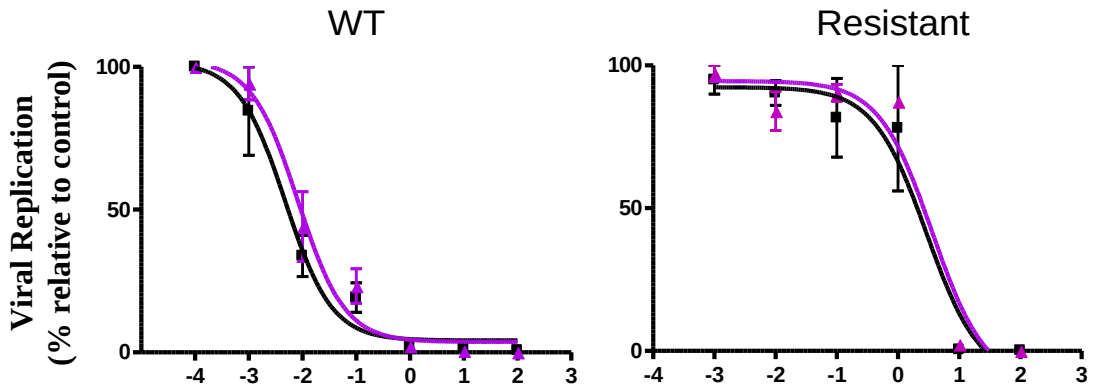

Figure 4. Dose-dependent inhibitory effect of DDI and DDI-Penta against WT and NRTI-resistant primary viral isolates, respectively. Dots represent the mean of three replicates ± SD. Lines represent the best-fit dose-response curves, calculated using GraphPad Prism 5.0 software. ■ DDI ▲DDI-Penta.

Table 2. Values of inhibitory concentrations (IC_{50}) of DDI, DDI-Penta and AZT against wild type and resistant HIV strains.

	IC_{50} (mM)[b]		
	DDI	**DDI-Penta**	**AZT**
WT[a]	0.003418	0.006485	0.0002162
R![c]	2.863	3.537	0.8291
Fold-R![d]	900X	600X	4000X

[a]WT: PBMCs infected with a Wild-Type HIV primary isolate.
[b]IC_{50} = concentration of drug that inhibited 50% of viral production.
[c]R! = PBMCs infected with a primary isolate presenting NRTI resistance-associated mutations.
[d]Fold-R! = Fold-resistance.

2.3. Molecular modeling studies

2.3.1. Molecular docking

To further study, if the anti-HIV performances of the prodrugs were related to their ratio of phosphorylation, the interaction with the enzyme ncN-II could be studied by molecular docking methods. Besides, the binding of DDI in its monophosphorylated form (DDI-MP) and that of the reported inhibitor AdiS were also analyzed and used as reference compounds. Table 3 shows the docking rank obtained together with the corresponding energetic components for the intermolecular interaction as calculated by the *Chemgauss4* force field.

Table 3. Energetic components derived from the molecular docking of the studied compounds.

Ligand	Rank	Tot. Score	VdW[b]	Elect.[c]	Prot. Des.[d]	Lig. Des.[e]
DDI-MP	1	-9.09	-6.39	-9.39	2.75	3.93
DDI-Hepta	2	-8.00	-9.24	-8.09	4.84	4.49
DDI-Hexa	3	-7.96	-11.33	-6.59	5.18	4.79
DDI-Penta	5	-7.66	-7.61	-8.45	4.05	4.35
DDI-Buta	6	-7.28	-10.83	-6.81	5.57	4.79
DDI-Etha	7	-7.11	-9.03	-4.58	3.58	2.93
DDI	8	-5.79	-5.57	-7.91	3.21	4.47
AdiS[a]	9	-5.15	-6.54	-4.52	2.69	3.23

[a] Anthraquinone-like inhibitor reported in ref [6].
[b] Van der Waals component obtained by molecular docking using the Chemgauss4 scoring function.
[c] Electrostatic component obtained by molecular docking using the Chemgauss4 scoring function.
[d] Protein desolvation component calculated using the Chemgauss4 scoring function.
[e] Protein desolvation component calculated using the Chemgauss4 scoring function.

As can be seen in table 3, DDI-MP exhibited the highest affinity for ncN-II (i.e. it was the first ranked ligand) which is in some way expected since this is the compound formed by the enzyme. When the energetic components were analyzed, a high stabilization derived from electrostatic interactions (-9.39) was calculated, while a minor contribution from van der Waals contacts (-6.39) was found. As Figure 5.a shows, this high stabilization is mainly caused by the interaction between the phosphate moiety of DDI-MP and the positively charged side chain ofGln453. Besides, an additional contribution is gained by a hydrogen bond formed with Tyr457. When the binding of the studied prodrugs was analyzed, all of them showed similar orientations within the catalytic site of the enzyme, with the following predicted affinities: DDI-Hepta>DDI-Hexa> DDI-Penta> DDI-Buta> DDI-Etha. The docking rank clearly followed the order of lipophilicity of the prodrugs that showed higher predicted affinities for the most lipophilic prodrug. Figure 5.b presents the intermolecular interaction pattern obtained for DDI-Hepta. Although all the studied prodrugs exhibited a similar binding mode, subtle differences were observed for DDI-Penta (Figure 5.c) in which a higher number of electrostatic interactions between the purine moiety of the prodrug and ncN-II are established. This observation is also supported by the higher electrostatic component calculated for DDI-Penta (-8.45) if compared to the rest of the prodrugs. When studying the binding of DDI to this receptor (plot not shown), it was observed that this drug exhibited a lower binding affinity than the prodrugs, mainly caused by a minor

VdW contribution. Finally, it is noteworthy that the AdiS inhibitor ranked in the last place among the whole set of compounds (Figure 6.d). The results obtained by molecular docking suggest that the newly synthesized prodrugs of DDI are able to occupy the catalytic site of ncN-II, establishing an intermolecular interaction with key aminoacid residues.

The above commented results have confirmed that the prodrugs of DDI can fit into the catalytic site of ncN-II; however, the rigid-body molecular docking techniques are not precise enough to definitively assess the time-dependent conformation of the studied inclusion complex and the corresponding evolution of intermolecular forces involved.[41-42] Although the docking methods are very powerful to predict the initial pose of the complex, they may then be subjected to further refinement by molecular dynamics methods, in which the flexibility of cnN-II is taken into account and the effect of temperature and solvent can also be modeled.

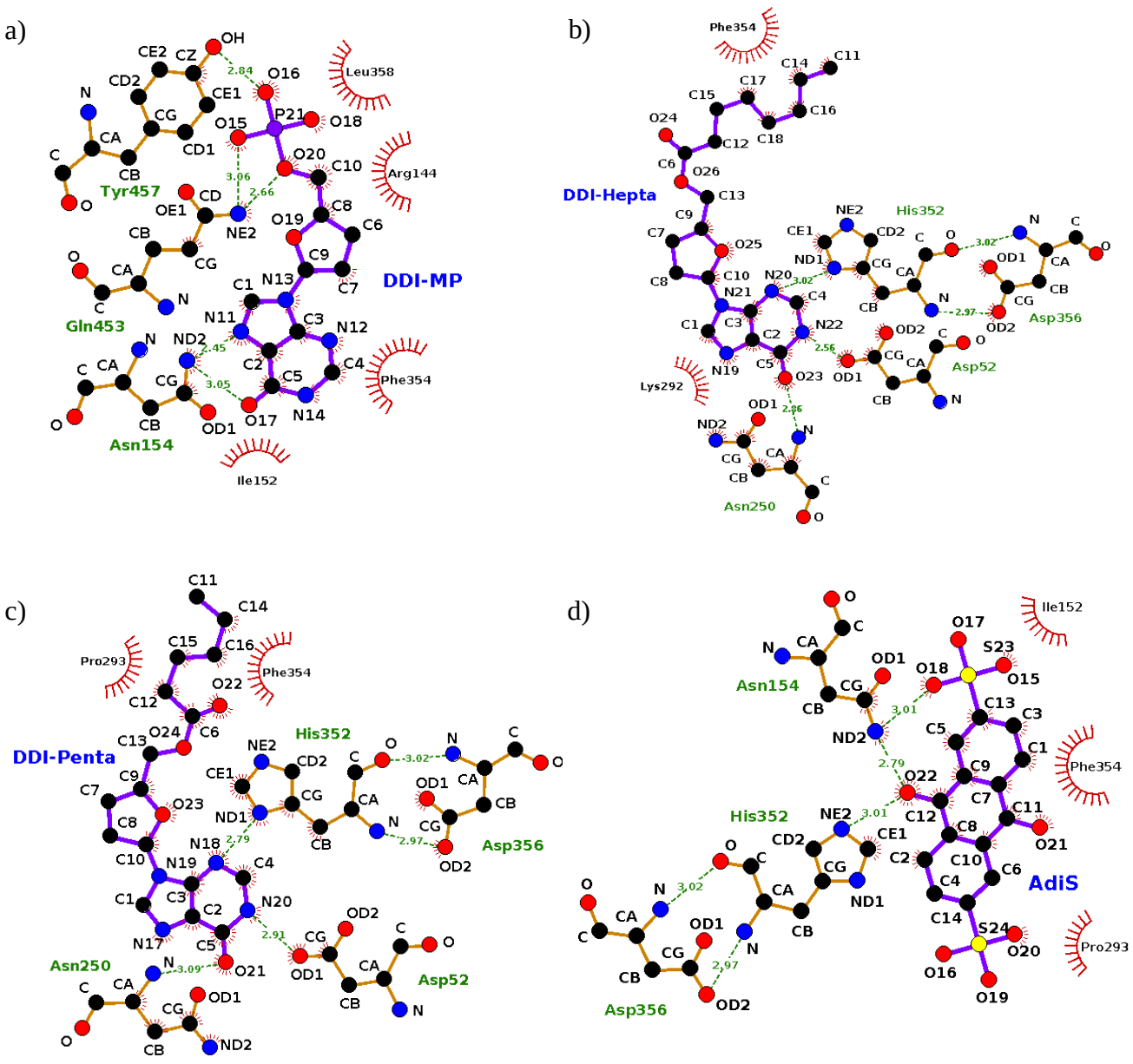

Figure 5. Intermolecular interactions predicted by molecular docking between ncN-II and: a) DDI-MP, b) DDI-Hepta, c) DDI-Penta and d) AdiS inhibitor.

2.3.2. Analysis of MD trajectories

After obtaining the corresponding MD production runs for the ligands: ncN-II complexes, their quality was checked by evaluation of their potential, kinetic and total energies (plots not shown). Structural properties were also measured in order to asses if the studied ligands remained bound into the corresponding binding site, with values of their root mean square deviation (RMSD) indicating that in all cases the ligand:cnN-II complexes remained stable throughout the simulated time (1 ns).

Table 4 presents the energetic components derived from the MMPBSA decomposition analysis performed throughout the whole production trajectory. In agreement with what was observed by molecular docking, DDI-MP exhibited the highest interaction energies, which is somehow expected since it constitutes the natural ligand of ncN-II. It is noteworthy that the binding of this compound is highly stabilized by electrostatic interactions (-593.84 Kcal/mol) which are mostly caused by the interaction of the ionized phosphate moiety with Arg144, Lys362 and Arg456. This observation suggests that this kind of interaction is the main driving force for the binding of ligands to the catalytic site. When the rest of the ligands were analyzed, the AdiS inhibitor appeared as the molecule with the second highest electrostatic component (-274.57 Kcal/mol), which was again caused by the interaction with the three above mentioned aminoacid residues. Due to the interaction between Lys359 and Lys362, DDI-Penta was the third ligand that exhibited the highest electrostatic interaction component (-262.16 kcal / mol). This observation suggests that DDI-Penta may be a ligand with a similar affinity for ncN-II as AdiS, which has a reported K_i of 2 mM,[6] and may be efficiently hydrolyzed and further phosphorylated by this enzyme. These results could be consistent with its high anti-HIV potency and diminished cytotoxicity. The rest of the studied prodrugs exhibited significantly lower electrostatic interaction components, a fact that seems to be caused by a less efficient complementarity of their three-dimensional conformation to the enzyme binding site, preventing the interaction with key aminoacid residues.

Table 4. Energetic decomposition analysis and component values derived from the molecular dynamics simulations of the studied compounds.

	Intermolecular interaction component (Kcal/mol)					
Ligand	**VdW[a]**	**Elect.[b]**	**Gas[c]**	**Pol. Solv.[d]**	**NP Solv.[e]**	**Total[f]**
DDI-MP	-27.26	-593.84	-621.10	551.37	-5.01	-74.74
DDI-Hepta	-49.68	-41.30	-90.98	60.10	-7.29	-38.17
DDI-Hexa	-49.76	-39.11	-88.88	57.24	-6.75	-38.38
DDI-Penta	-24.79	-262.16	-286.95	258.19	-4.34	-28.76
DDI-Buta	-43.61	-95.93	-139.54	90.69	-6.16	-55.01
DDI-Etha	-33.95	-37.50	-71.45	48.83	-5.52	-28.13
DDI	-26.13	-37.32	-63.45	48.55	-4.43	-19.32
AdiS	-22.14	-274.57	-296.71	267.92	-4.66	-33.45

[a] Van der Waals interaction energetic component.
[b] Electrostatic interaction energetic component.
[c] Total interaction energy in the gas phase (VdW + Elect).
[d] Total polar solvation energy.
[e] Total non-polar solvation energy.
[f] Total interaction energy calculated by the MMPBSA method.

3. Conclusion

The synthesis of five 5´-*O*-2´,3´-dideoxydidanosine prodrugs with the further quantitation of their *in vitro* anti-HIV activity in PBMCs and associated cytotoxicity has been described. These studies have shown the utility of the carbonate linkage in creating prodrugs from DDI and also indicated how the physical-chemical properties of this drug have been substantially modified to produce different compounds with increased lipophilicities and good antiviral performance (inhibitory potency and low cytotoxicity).

The outstanding increase in the selective index of DDI-Penta compared to that of the parent drug could be related to the ability of this prodrug to efficiently bind to ncN-II, which would in turn generate higher intracellular levels of DDI-MP. Besides, based on their higher calculated lipophilicities, we believe that an improved permeability through the cell membrane would aid in reaching higher concentrations of these prodrugs within the target cells.

Founded on the above commented aspects, the use of a carbonate linkage at the 5'-OH position of DDI combined with the use of *n*-alcohols appears to be a very promising strategy to enhance the potency and security of this NRTI. Among the studied prodrugs, DDI-Penta outstands as the most promising candidate for further evaluations.

4. Materials and Methods

4.1. Chemistry

All chemicals, reagents and solvents were of analytical grade. The nucleoside 5´-*O*-2´,3´-dideoxyinosine (Didanosine, DDI, **1**), a generous gift from Filaxis Laboratory (Buenos Aires, Argentina), and *N*,*N*-carbonyldiimidazole (>97% purity, Sigma) were used without purification. Dimethylformamide (DMF) was dried over 4Å molecular sieves. All solid reagents were dried for several hours under high vacuum. Thin layer chromatography (TLC) was performed on Merck Sil G/UV_{254} silica gel plates with fluorescent indicator, and the spots were visualized under 254 nm illumination. All glassware was oven-dried at 130 ºC overnight, and cooled in a desiccator over anhydrous $CaSO_4$. All ^{1}H NMR and ^{13}C NMR spectra were recorded on a Bruker Avance 400, Ultrashield, Frecuency of ^{1}H NMR 400.16 MHz and that of ^{13}C NMR 100.62 Hz, Dual BBI Probe, at 25 ºC using DMSO-d_6 (99.8%, Merck) as solvent. The assignment of all exchangeable protons (OH, NH) was confirmed by the addition of D_2O (99.9%, Sigma). Chemical shift values are reported in parts per million (δ) relative to tetramethylsilane (TMS); internal standard and coupling constants (*J*) are given in Hertz (Hz). The splitting pattern abbreviations are as follows: s, singlet; t, triplet; m, multiplet; and dd, doublet of doublet. All ^{13}C NMR spectra were proton-decoupled confirmed by using the 135º DEPT technique as well as COSY (^{1}H–^{1}H) and HSQC (^{1}H–^{13}C) correlation. Infrared spectra were recorded on a Bruker IFS 66 FTIR-spectrophotometer in the 4000–400 cm^{-1} range using the KBr pellet technique. Raman spectra were obtained with a Spex-Ramalog double monochromator spectrometer, using the 514.5 nm line of an argon ion laser for excitation. The rotating disk technique was used to avoid burning of the compound by the laser light. High resolution mass spectrometry (HRMS) was performed in a Bruker MICROTOF-Q II, equipped with an electrospray (ESI) interface configured in positive mode. Ultraviolet spectrophotometric (UV) studies were carried out with a Shimadzu Model UV-160A spectrophotometer with 1 cm quartz cells.

4.1.1. General procedure for the synthesis of 5´-*O*-carbonates of DDI

1.2 eq. of *N*,*N*-carbonyldiimidazole (170 mg; 1 mmol 1.2 eq.) was added under N_2 stream to 1 eq. (200 mg, 0.847 mmol, 1 eq.) of **1** in dried DMF (2.0 mL). The reaction mixture was stirred at 40 ºC for 1h leading to an intermediate of DDI (DDI-5´-CI). The progress of the reaction was monitored by TLC using CH_2Cl_2:MeOH, 5:5 v/v as a mobile phase. Afterward, the aliphatic alcohol (1.5 eq.) was added, and the reaction mixture was then maintained in the same conditions until total conversion of DDI-5´-CI with the formation of the corresponding carbonate product. The solvent was removed under reduced

pressure, and the residual oil was dissolved in CH_2Cl_2 (1 x 20 mL). The organic phase was successively extracted with water (3 x 20 mL) and then dried over Na_2SO_4, filtrated and evaporated to give the crude product. Finally, **4-8** were recrystallized from CH_2Cl_2-hexane. R_f values were determined using CH_2Cl_2:MeOH (5:5) as a mobile phase.

2´, 3´-dideoxyinosine-5´-yl *O*-ethyl carbonate (4, DDI-Etha)

According to the general procedure, by adding ethanol (0.148 mL, 2.617 mmol, 3 eq.), the title compound **4** was obtained as a white solid. Yield: 224 mg (90%); R_f: 0.45; MW: 308.2.

^{1}H-NMR (DMSO-d_6): δ 12.37 (s, 1H, H-1), 8.25 (s, 1H, H-8), 8.02 (s, 1H, H-2), 6.22 (dd, *J* = 6.6, 3.0 Hz, 1H, H-1´), 4.30 (m, 1H, H-4'), 4.20 (m, 2H, H-5'), 4.03 (m, 2H, H-2"), 2.40 (m, 1H, H-2'$_a$), 2.20 (m, 1H, H-2'$_b$), 2.05 (m, 2H, H-3'), 0.90 (t, 3H, H-3"). **^{13}C-NMR** (DMSO-d_6): δ 158.2 (C, C-4), 154.97 (C(O), C-1"), 148.20 (C(O), C-6), 146.17 (CH, C-2), 138.55 (CH, C-8), 124.82 (CH, C-5), 84.82 (CH, C-1'), 78.78 (CH_2, C-4'), 69.06 (CH_2, C-5'), 67.82 (CH_2, C-2"), 31.72 (CH_2, C-2'), 12.87 (CH_3, C-3") . **UV** (H_2O)/nmλ_{max}: 248.2. **IR** (KBr disk) ν_{max}: 3100.0-3400.0 (NH), 2900.8 (CH_2, C=C), 1760.1 (OC(O)O), 1700.6 (CO) cm^{-1}. MS (ESI): m/z 331.1 (M+23). $C_{13}H_{16}N_4O_5$ (308.2).

2´,3´-dideoxyinosine-5´-yl *O*-butyl carbonate (5, DDI-Buta)

In accordance with the general procedure, by adding *n*-butanol (0.239 mL, 2.617 mmol, 3 eq.), the title compound **5** was obtained as a white solid. Yield: 257 mg (90%); R_f: 0.56; MW: 336.2.

^{1}H-NMR (DMSO-d_6): δ 12.36 (s, 1H, H-1), 8.22 (s, 1H, H-8), 8.06 (s, 1H, H-2), 6.23 (dd, *J* = 6.5, 3.2 Hz, 1H, H-1´), 4.29 (m, 1H, H-4'), 4.20 (m, 2H, H-5'), 4.02 (t, *J* = 6.8 Hz, 2H, H-2"), 2.45 (m, 1H, H-2'$_a$), 2.14 (m, 1H, H-2'$_b$), 2.05 (m, 2H, H-3'), 1.54 (m, 2H, H-3") 1.31 (m, 2H, H-4"), 0.87 (t, *J* = 7.2 Hz, 3H, H-5"). **^{13}C-NMR** (DMSO-d_6): δ 157.05 (C, C-4), 154.97 (C(O), C-1"), 148.20 (C(O), C-6), 146.17 (CH, C-2), 138.55 (CH, C-8), 124.82 (CH, C-5), 84.82 (CH, C-1'), 78.78 (CH_2, C-4'), 69.06 (CH_2, C-5'), 67.82 (CH_2, C-2"), 31.72 (CH_2, C-2'), 30.55 (CH_2, C-3"), 26.43 (CH_2, C-3'), 18.83 (CH_2, C-4"), 13.95 (CH_3, C-5") . **UV** (H_2O)/nmλ_{max}: 248.2. **IR** (KBr disk) ν_{max}: 3100.0-3400.0 (NH), 2900.2 (CH_2, C=C), 1760.5 (OC(O)O), 1702.6 (CO) cm^{-1}. MS (ESI): m/z 337.1 (M+1). $C_{15}H_{20}N_4O_5$ (336.2).

2´,3´-dideoxyinosine-5´-yl *O*-pentyl carbonate (6, DDI-Penta)

In line with the general procedure, by adding *n*-pentanol (0.284 mL, 2.617 mmol, 3 eq.), the title compound **6** was obtained as a white solid. Yield: 279 mg (94%); R_f: 0.59; MW: 350.2.

^{1}H-NMR (DMSO-d_6): δ 12.36 (s, 1H, H-1), 8.20 (s, 1H, H-8), 7.84 (s, 1H, H-2), 6.23 (dd, *J* = 6.5, 3.2 Hz, 1H, H-1´), 5.40 (m, 1H, H-4'), 4.10 (m, 2H, H-2"), 3.47 (m, 1H, H-2'$_a$), 3.20 (m, 1H, H-2'$_b$), 1.60 (m, 3H, H-3'), 1.54 (m, 2H, H-3") 1.32 (m, 4H, H-4" H-5"), 0.88 (t, *J* = 6.6 Hz, 3H, H-6"). **^{13}C-NMR** (DMSO-d_6): δ 157.05 (C, C-4), 154.97 (C(O), C-1"), 148.20 (C(O), C-6), 146.17 (CH, C-2), 138.55 (CH, C-8), 124.82 (CH, C-5), 84.82 (CH, C-1'), 78.78 (CH_2, C-4'), 69.06 (CH_2, C-5'), 67.82 (CH_2, C-2"), 31.72 (CH_2, C-2'), 30.55 (CH_2, C-3"), 26.43 (CH_2, C-3'), 18.83 (CH_2, C-4"), 15.41 (CH_2, C-4"), 13.25 (CH_3, C-6"). **UV** (H_2O)/nmλ_{max}: 248.2. IR (KBr disk) ν_{max}: 3110.2-3400.0 (NH), 2910.6 (CH_2, C=C), 1760.5 (OC(O)O), 1702.6 (CO) cm^{-1}. MS (ESI): m/z 350.2 (M+1). $C_{16}H_{22}N_4O_5$ (351.1).

2´,3´-dideoxyinosine-5´-yl *O*-hexyl carbonate (7, DDI-Hexa)

According to the general procedure, the addition of *n*-hexanol (0.327 mL, 2.617 mmol, 3 eq.) afforded the title compound **7** as a white solid. Yield: 271 mg (88 %); R_f: 0.63; MW: 364.2.

^{1}H-NMR (DMSO-d_6): δ 12.34 (s, 1H, H-1), 8.20 (s, 1H, H-8), 8.03 (s, 1H, H-2), 6.20 (dd, *J* = 6.5, 3.2Hz, 1H, H-1´), 4.28 (m, 1H, H-4'), 4.18,(m, 2H, H-5'), 4.02 (t, *J* = 6.5 Hz, 2H, H-2"), 2.45 (m, 1H, H-2'$_a$), 2.08 (m, 1H, H-2'$_b$), 1.55 (m, 4H, H-3' H-3"), 1.30 (m, 6H, H-4" H-5" H-6"), 0.75 (t, *J* = 5.1 Hz, 2H, H-7"). **^{13}C-NMR** (DMSO-d_6): δ 157.05 (C, C-4), 154.97 (C(O), C-1"), 148.19 (C(O), C-6), 146.17 (CH, C-2), 138.54 (CH, C-8), 124.82 (CH, C-5), 84.83 (CH, C-1'), 78.78 (CH_2, C-4'), 69.09 (CH_2, C-5'), 68.12 (CH_2, C-2"), 31.74 (CH_2, C-2'), 31.24 (CH_2, C-3"), 28.47 (CH_2, C-3'), 26.43 (CH_2, C-4"), 25.23 (CH_2, C-5"), 22.41 (CH_2, C-6"), 14.31 (CH_3, C-7"). **UV** (H_2O)/nmλ_{max}: 248.2. IR (KBr disk) ν_{max}: 3108.2-3400.0 (NH), 2910.6 (CH_2, C=C), 1772.6 (OC(O)O), 1714.8 (CO) cm^{-1}. MS (ESI): m/z 365.1 (M+1). $C_{17}H_{24}N_4O_5$ (364.2).

2´,3´-dideoxyinosine-5´-yl O-heptylcarbonate (8, DDI-Hepta)

In agreement with the general procedure, the addition of *n*-heptanol (0.366 mL, 2.617 mmol, 3 eq.) afforded the title compound **8** as a white solid. Yield: 256 mg (80 %); R_f: 0.65; MW: 378.2.

^{1}H-NMR (DMSO-d_6): δ 12.35 (s, 1H, H-1), 8.22 (s, 1H, H-8), 8.15 (s, 1H, H-2), 6.18 (dd, *J* = 6.5, 3.2Hz, 1H, H-1´), 4.28 (m, 1H, H-4'), 4.18,(m, 2H, H-5'), 4.02 (t, *J* = 6.5 Hz, 2H, H-2"), 2.45 (m, 1H, H-2'$_a$), 2.08 (m, 1H, H-2'$_b$), 1.55 (m, 4H, H-3' H-3"), 1.35 (m, 8H, H-4" H-5" H-6" H-7"), 0.63 (t, *J* = 5.0 Hz, 2H, H-8"). **^{13}C-NMR** (DMSO-d_6): δ 157.05 (C, C-4), 154.97 (C(O), C-1"), 148.19 (C(O), C-6), 146.17 (CH, C-2), 138.54 (CH, C-8), 124.82 (CH, C-5), 84.83 (CH, C-1'), 78.78 (CH_2, C-4'), 69.09 (CH_2, C-5'), 68.12 (CH_2, C-2"), 31.74 (CH_2, C-2'), 31.24 (CH_2, C-3"), 28.47 (CH_2, C-3'), 26.43 (CH_2,

C-4"), 25.23 (CH_2, C-5"), 22.41 (CH_2, C-6"), 14.31 (CH_2, C-7"), 14.20 (CH_2, C-8"). **UV** (H_2O)/nmλ_{max}: 248.2. IR (KBr disk) ν_{max}: 3108.2-3400.0 (NH), 2910.6 (CH_2, C=C), 1772.6 (OC(O)O), 1714.8 (CO) cm^{-1}. MS (ESI): m/z 379.0 (M+1). $C_{18}H_{26}N_4O_5$ (378.2).

4.2. Antiviral Activity Assays

4.2.1. Cells and HIV-1 strains

Peripheral blood mononuclear cells (PBMC) were isolated by Ficoll–Hypaque (Amersham Pharmacia Biotech, Sweden) gradient centrifugation from peripheral blood of HIV-1seronegative patients and cultured at 37°C in RPMI-1640 medium (Sigma-Aldrich, USA) supplemented with 2 mM-glutamine (Gibco BRL, USA), 100 U/ml penicillin (Gibco BRL), 100 mg/ml streptomycin (GibcoBRL), 10% fetal bovine serum (FBS, Gibco BRL) and 10 U/ml interleukin-2 (IL-2, BD Biosciences, USA). Prior to infection, PBMCs were stimulated with 0.1% phytohaemagglutinin (PHA) for 3 days.

Stock of HTLV-IIIB strain of HIV-1 was derived from chronically infected H9 cells. Two different primary HIV isolates were obtained by co-culture of PBMCs from HIV-infected and HIV non-infected donors. Nucleotide sequencing of *pol* gene revealed that one of the isolates showed a WT sequence (WT isolate) while the other (NRTI-resistant isolate) harbored several mutations associated with resistance to nucleoside RT inhibitors (D67N, T69D, K70R, A98G, V118I, M184V, T215F and K219Q).

4.2.2. Antiviral activity and cytotoxicity assays

PBMCs were infected at 6.45×10^5 $TCID_{50}/10^6$ cells for 2 h at 37°C. After infection, cells were washed and dispensed in a 96-well plate in the presence of 10-fold serial dilutions of compounds. The experiments were performed in triplicate. Untreated wells and wells treated with DDI were also monitored as controls of antiviral activity. Culture medium was changed on the fourth day maintaining the original concentration of the drug. On the seventh day, supernatant fluids were harvested and production of p24 antigen was subsequently evaluated using a commercial enzyme linked immunosorbent assay (ELISA) (Vironostika, The Netherlands). Based on p24 quantitation, the dose that inhibited 50% of the viral production (IC_{50}) was determined.

Cytotoxicity studies on uninfected PBMCs were performed in parallel in order to determine the concentration of the drug that inhibited 50% of cell growth ($CCID_{50}$). Cellular viability was evaluated

by trypan blue (TB) staining and subsequent counting of viable cells on Neubauer chamber. Assays were performed in triplicate.[30, 34, 43]

Once both parameters ($CCID_{50}$ and IC_{50}) were obtained, the selectivity index (SI), which is defined as $CCID_{50}/IC_{50}$, was determined. When assaying NRTI-resistant virus isolate, fold-resistance (fold-R!) was calculated as the ratio between the IC_{50} obtained in Resistant-infected and WT-infected cultures. Results obtained in cultures treated with AZT are also shown as reference.

4.3. Molecular modeling studies

4.3.1. Molecular docking

The structures corresponding to the studied ligands were constructed using the Gabedit graphical interface,[44] and were afterwards subjected to energy minimization using semi-empirical and *ab-initio* methods as implemented in the Gaussian03 package.[45] The minimum energy conformation was then subjected to ionization and tautomers analysis considering a pH of 7.0 by applying the algorithms implemented in the MOKA software (Molecular Discovery Ltd.),[46-47] with the resulting structure being used as a starting point to generate a conformer database intended for the rigid-body docking protocols. The OMEGA software was used to generate this database,[48-49] applying an energy threshold of 10 Kcal and assigning *BCC* system charges to each conformer to model the corresponding intermolecular forces during docking runs.

The receptor model used for docking assays corresponded to the crystal structure of ncN-II in complex with an anthraquinone derived inhibitor (AdiS), which has been recently reported by Jordheim*et al*.[6] The structure was retrieved from the Protein Databank (pdb code: 4H4B). Before performing the docking runs, crystallographic water molecules present in a 6Å radius from the ligand were retained. A docking box of 10000 $Å^3$ was generated and centered on AdiS, with standard ionization states being considered for the rest of the protein.

The ligands conformer libraries were docked to the above mentioned receptor using a fast rigid exhaustive docking approach as implemented in the *FRED* software,[50-51] with the corresponding docked poses being scored using the *Chemgauss4* function as implemented in the software package. The lowest energy binding pose was selected, analyzed and subjected to posterior molecular dynamics (MD) studies. Visualization and analysis of intermolecular interactions were performed using the VIDA, VMD and LigPlus software packages.[52-53]

4.3.2. Molecular dynamics (MD) simulations

MD simulations were performed using the Amber12 software package.[54] Charges and parameters of ligands were assigned from the *GAFF* atomic force-field,[55]while the parameters for the receptor corresponded to the *ff03ua* force field.[56] Initial coordinates of the corresponding complexes were obtained by the molecular docking procedures described above, and simulated under implicit solvent conditions. The protocol applied included the following stages: a) minimization stage (10000 steps), b) heating phase (20 ps, target temperature 300 K) performed under constant volume conditions, c) an equilibration step (200 ps) at constant volume and temperature (300 K) conditions and finally d) a production run (1 ns) obtained at constant pressure and temperature (300 K). In all cases, an integration time step of 2 fs was used applying the SHAKE algorithm to restrain the bonds involving the hydrogen atoms. Analysis over the MD trajectories were applied using the *Ccptraj* module of Amber12, while total and per-residue energetic decomposition analysis were performed using the Molecular Mechanics Poisson-Bolzmann Surface Area (MM-PBSA) approach.[57]

Molecular dynamics trajectories were obtained using CUDA designed code (pmemd.cuda). The computational facilities were provided by the GPGPU Computing group of the Facultad de Matemática, Astronomía y Física (FAMAF), Universidad Nacional de Córdoba, Argentina.

ACKNOWLEDGMENTS

The authors gratefully acknowledge Secretaría de Ciencia y Técnica de la Universidad Nacional de Córdoba (SECYT-UNC), Consejo Nacional de Investigaciones Científicas y Tecnológicas (CONICET) and Fondo para la Investigación Científica y Tecnológica (FONCYT) of Argentina for financial support. The authors also wish to express their sincere thanks to L. Alassia (FILAXIS Laboratories, Buenos Aires, Argentina) for supplying didanosine. S.R. and M.S.G. acknowledge receipt of fellowships granted by CONICET. Mario A. Quevedo would also like to acknowledge the GPGPU Computing Group and Dr. Nicolás Wolovick from the Facultad de Matemática, Astronomía y Física (FAMAF), Universidad Nacional de Córdoba, Argentina, for providing access to computing resources. Gloria Bonetto's assistance in NMR data analyses is also gratefully acknowledged.

REFERENCES

1 S. Broder, *Antiviral Res.*, 2010, **85**, 1-18.

2 Joint United Nations Programme on HIV/AIDS (UNAIDS). Global report: UNAIDS report on the global AIDS epidemic 2010. Switzerland. 2010. Available on: http://www.unaids.org/globalreport/documents/20101123_GlobalReport_full_en.pdf.

3 H. Mitsuya, S. Broder, *Proc. Natl. Acad. Sci. U. S. A.*, 1986, **83**, 1911-1915.

4 X. Tan, C.K. Chu, F.D. Boudinot, *Adv. Drug Deliv. Rev.*, 1999, **39**, 117-151.

5 F. Gallier, P. Lallemand, M. Meurillon, L. P. Jordheim, C. Dumontet, C. Périgaud, C. Lionne, S. Peyrottes, L. Chaloin, *PLoS Computational Biology*, 2011, **7**.

6 L. P. Jordheim, Z. Marton, M. Rhimi, E. Cros-Perrial, C. Lionne, S. Peyrottes, C. Dumontet, N. Aghajari, L. Chaloin, *Biochem. Pharmacol.*, 2013, **85**, 497-506.

7 M. Lalanne, H. Khoury, A. Deroussent, N. Bosquet, H. Benech, P. Clayette, P. Couvreur, G. Vassal, A. Paci, K. Andrieux, *Int. J. Pharm.*, 2009, **379**, 235-243.

8 E. De Clercq, *Curr. Opin. Pharmacol.*, 2010, **10**, 507-515.

9 E. De Clercq, *Antiviral Res.*, 2010, **85**, 19-24.

10 B. D. Anderson, B. L. Hoesterey, D. C. Baker, R. E. Galinsky, *J. Pharmacol. Exp. Ther.*, 1990, **253**, 113-118.

11 A. Igoudjil, K. Begriche, D. Pessayre, B. Fromenty,*Anti-Infective Agents in Med Chem*, 2006, **5**, 273-292.

12 A.G. Marcelin, P. Flandre, J. Pavie, N. Schmidely, M. Wirden, O. Lada, D. Chiche, J. M. Molina, V. Calvez, *Antimicrob. Agents Chemother.*, 2005, **49**, 1739-1744.

13 L. I. Wiebe, E. E. Knaus, *Adv. Drug Deliv. Rev.*, 1999, **39**, 63-80.

14 T. Calogeropoulou, A. Detsi, E. Lekkas, M. Koufaki, *Curr Top Med Chem*, 2003, **3**, 1467-1495.

15 F. J. Piacenti,*Pharmacotherapy*, 2006, **26**, 1111-1133.

16 C. Anastasi, P. Vlieghe, O. Hantz, O. Schorr, C. Pannecouque, M. Witvrouw, E. De Clercq, P. Clayette, N. Dereuddre-Bosquet, D. Dormont, F. Gondois-Rey, I. Hirsch, J. L. Kraus, *Bioorg. Med. Chem. Lett.*, 2003, **13**, 2459-2463.

17 N. Bodor, J. J. Kaminski, Prodrugs and Site-Specific Chemical Delivery Systems. 1987, Vol. 22, pp 303-313.

18 N. Bodor, M. E. Brewster, *Pharmacol. Ther.*, 1982, **19**, 337-386.

19 P. Vlieghe, F. Bihel, T. Clerc, C. Pannecouque, M. Witvrouw, E. De Clercq, J. P. Salles, J. C. Chermann, J. L. Kraus,*J.Med. Chem.*, 2001, **44**, 777-786.

20 K. Parang, L. I. Wiebe, E. E. Knaus, *Curr. Med. Chem.*, 2000, **7**, 995-1039.

21 S. Høyem, S. Bruheim, G. Mælandsmo, M. Standal, D. E. Olberg, B. Brudeli, A. Åsberg, J. Klaveness, P. Rongved, *Eur. J. Med. Chem.*, 2009, **44**, 3874-3879.

22 S. Ravetti, M. S. Gualdesi, M. C. Briñón, *J. of Liq. Chrom. & Rel. Tech.*, 2008, **31**, 1014-1032.

23 G. N. Moroni, M. A. Quevedo, S. Ravetti, M. C. Briñón, *J. of Liq. Chrom. & Rel. Tech.*, 2002, **25**, 1345-1365.

24 M. A. Raviolo, M. C. Briñón, *J. of Liq. Chrom. & Rel. Tech.*, 2005, **28**, 2195-2209.

25 D. Sriram, N. Srichakravarthy, T. R. Bal, P. Yogeeswari, *Biomed. Pharmacother.*, 2005, **59**, 452-455.

26 D. Sriram, P. Yogeeswari, N. Srichakravarthy, T. R. Bal, *Bioorg. Med. Chem. Lett.*, 2004, **14**, 1085-1087.

27 D. Sriram, P. Yogeeswari, N. S. Myneedu, V. Saraswat, *Bioorg. Med. Chem. Lett.*, 2006, **16**, 2127-2129.

28 M. Motura, H. Salomón, G. N. Moroni, M. Wainberg, M. C. Briñon,*Nucleos. Nucleot. Nucl.*, 1999, **18**, 337-351.

29 N. Mourier, M. Camplo, G. S. Della Bruna, F. Pellacini, D. Ungheri, J. C. Chermann, J. L. Kraus, *Nucleos., Nucleot. Nucl.*, 2000, **19**, 1057-1091.

30 S. Ravetti, M. S. Gualdesi, J. S. Trinchero-Hernández, G. Turk, M. C. Briñón, *Bioorg. Med. Chem.*, 2009, **17**, 6407-6413.

31 M. A. Raviolo, J. S. Trinchero-Hernández, G. Turk, M. C. Briñón, *J. Braz.Chem. Soc.*, 2009, **20**, 1870-1877.

32 G. N. Moroni, P. M. Bogdanov, M. C. Briñón, *Nucleos. Nucleot. Nucl.*, 2002, **21**, 231-241.

33 M. I. Motura, G. N. Moroni, S. A. Teijeiro, H. Salomón, M. C. Briñón, *Nucleos.Nucleot.Nucl.*, 2002, **21**, 217-230.

34 G. Turk, G. N. Moroni, S. Pampuro, M. C. Brión, H. Salomón, *Int. J. Antimicrob. Agents*, 2002, **20**, 282-288.

35 Z. Gu, H. Salomon, J. M. Cherrington, A. S. Mulato, M. S. Chen, R. Yarchoan, A. Foli, K. M. Sogocio, M. A. Wainberg, *Antimicrob. Agents Chemother.*, 1995, **39**, 1888-1891.

36 K. Hammer, J. Hatlelid, M. Grøtli, J. Arukwe, J. Klaveness, F. Rise, K. Undheim, *Acta Chem. Scand.*, 1996, **50**, 609-622.

37 D. Gagey, S. Ravetti, E. F. Castro, M. S. Gualdesi, M. C. Briñon, R. H. Campos, L. V. Cavallaro, *Int. J. Antimicrob. Agents*, 2010, **36**, 566-569.

38 S. P. Rannard, N. J. Davis, *Org. Lett.*, 1999, **1**, 933-936.

39 S. P. Rannard, N. J. Davis, *J. Am. Chem. Soc.*, 2000, **122**, 11729-11730.

40 M. N. Nassar, T. Chen, M. J. Reff, S. N. Agharkar, 1993; vol. 22, pp 185-227.

41 A. Zoppi, M. A. Quevedo, M. R. Longhi, *Bioorg. Med. Chem.*, 2008, **16**, 8403-8412.

42 A. Zoppi, M. A. Quevedo, A. Delrivo, M. R. Longhi, *J. Pharm. Sci.*, 2010, **99**, 3166-3176.

43 J. Trinchero, N. M. A. Ponce, O. L. Córdoba, M. L. Flores, S. Pampuro, C. A. Stortz, H. Salomón, G. Turk, *Phytother. Res.*, 2009, **23**, 707-712.

44 A. R. Allouche, A. Gabedita, *J. Comput. Chem.*, 2011, **32**, 174-182.

45 M. J. Frisch, G. W. Trucks, H. B. Schlegel, G. E. Scuseria, M. A. Rob,J. R. Cheeseman J. A. jr. Montgomery, T. Vreven, K. N. Kudin, J. C. Burant, J. M. Millam, S. S. Iyengar, J. Tomasi, V. Barone, B. Mennucci, M. Cossi, G. Scalmani, N. Rega, G. A. Petersson, H. Nakatsuji, M. Hada, M. Ehara, K. Toyota, R. Fukuda, J. Hasegawa, M. Ishida, T. Nakajima, Y. Honda, O. Kitao, H. Nakai, M. Klene, X. Li, J. E. Knox, H. P. Hratchian, J. B. Cross, V. Bakken, C. Adamo, J. Jaramillo, R. Gomperts, R. E. Stratmann, O. Yazyev, A. J. Austin, R. Cammi, C. Pomelli, J. W. Ochterski, P. Y. Ayala, K. Morokuma, G. A. Voth, P. Salvador, J. J. Dannenberg, V. G. Zakrzewski, S. Dapprich, A. D. Daniels, M. C. Strain, O. Farkas, D. K. Malick, D. K. Rabuck, K. Raghavachari, J. B. Foresman, J. V. Ortiz, Q. Cui, A. G. Baboul, S. Clifford, J. Cioslowski, B. B. Stefanov, G. Liu, A. Liashenko, P. Piskorz, I. Komaromi, R. L. Martin, D. J. Fox, T. Keith, M. A. Al-Laham, C. Y. Peng, A. Nanayakkara, M. Challacombe, P. M. W. Gill, B. Johnson, W. Chen, M. W. Wong, C. Gonzalez, J. A. Pople, Gaussian 03. 2003.

46 F. Milletti, L. Storchi, G. Sforna, G. Cruciani, *J. Chem. Inf. Model.*, 2007, **47**, 2172-2181.

47 F. Milletti, L. Storchi, G. Sfoma, S. Cross, G. Cruciani, *J. Chem. Inf. Model.*, 2009, **49**, 68-75.

48 Omega.2.4.3 OpenEye Scientific Software, Santa Fe, NM http://www.eyesopen.com.

49 P. C. D. Hawkins, A. G. Skillman, G. L. Warren, B. A. Ellingson, M. T. Stahl, *J. Chem. Inf. Model.*, 2010, **50**, 572-584.

50 Fred.3.0.0 OpenEye Scientific Software, Santa Fe, NM http://www.eyesopen.com.

51 M. McGann, *J. Comput. Aided Mol. Des.*, 2012, **8**, 1-10.

52 VIDA.4.2.1 OpenEye Scientific Software, Santa Fe, NM http://www.eyesopen.com.

53 W. Humphrey, A. Dalke, K. Schulten, *J. Mol. Graph.*, 1996, **14**, 33-38.

54 D. A. Case, T. E. Cheatham Iii, T. Darden, H. Gohlke, R. Luo, K. M. Merz Jr, A. Onufriev, C. Simmerling, B. Wang, R. J. Woods, *J. Comput. Chem.*, 2005, **26**, 1668-1688.

55 J. Wang, R. M. Wolf, J. W. Caldwell, P. A. Kollman, D. A. Case, *J. Comput. Chem.*, 2004, **25**, 1157-1174.

56 L. Yang, C. H. Tan, M. J. Hsieh, J. Wang, Y. Duan, P. Cieplak, J. Caldwell, P. A. Kollman, R. Luo, *J. Phys. Chem. B.*, 2006, **110**, 13166-13176.

57 B. Kuhn, P. Gerber, T. Schulz-Gasch, M. Stahl, *J. Med. Chem.*, 2005, **48**, 4040-4048.